Available online at www.sciencedirect.com
SCIENCE DIRECT®
PERGAMON
Computers and Structures 81 (2003) 1359–1374
Computers & Structures
www.elsevier.com/locate/compstruc

Impact simulation and full scale crash testing of a low profile concrete work zone barrier

Gary R. Consolazio *, Jae H. Chung, Kurtis R. Gurley [1]

Department of Civil and Coastal Engineering, University of Florida, P.O. Box 116580, Gainesville, FL 32611, USA

Received 9 July 2002; accepted 23 December 2002

Abstract

The development of a new low profile portable concrete barrier system for use in roadside work zone environments is presented. By making extensive use of non-linear dynamic finite element impact simulation, several cycles of concept refinement were carried out using simulation rather than expensive full scale crash testing. Issues such as ensuring stable vehicle redirection during impact, properly accounting for frictional effects (and associated energy dissipation), and monitoring system energy parameters are discussed together with corresponding example simulations. Results obtained from full scale crash testing of the barrier validate the simulation methodology and demonstrate successful barrier performance.

Keywords: Portable barrier; Work zone; Impact simulation; Friction; Energy dissipation; Hourglass energy

1. Introduction

In the past, the development of new roadside safety hardware systems such as railings, barriers, and energy absorbing crash cushions typically required iterative cycles of conceptual design and full scale vehicle crash testing. Much of the conceptual design process was based on sound understanding of engineering and mechanics principles, previous development experience, and intuition. However, with only these tools available, several cycles of concept development and crash testing were usually required to arrive at a successful design. Given the setup time and costs involved in full scale crash testing, and the matrix of testing conditions that must be examined for system approval [1], this process can be quite costly as well as time consuming.

Over the past decade, the roadside hardware design process has changed substantially as non-linear dynamic finite element analysis (FEA) has found increasing application. A substantial portion of conceptual design can now be performed using computational simulation rather than experimental testing. Such use of simulation can result in more rapid system development, improved system performance, and reduced development costs. Ultimately, such systems must still be subjected to full scale crash testing to validate and certify their integrity. However, far fewer cycles of development and testing are required if simulation results can be relied upon to identify design flaws that degrade system performance.

This paper describes the process by which numeric simulation was recently used to carry out conceptual development of a new temporary concrete work zone barrier. Extensive use was made of the non-linear explicit dynamic finite element simulation code LS-DYNA [2] to identify and correct design flaws early in the concept development stage. After arriving at what was considered to be a viable system design, full scale physical crash testing was carried out to verify the successful performance of the system.

* Corresponding author. Tel.: +1-352-392-9537x1510; fax: +1-352-392-3394.
E-mail addresses: grc@ce.ufl.edu (G.R. Consolazio), kgurl@ce.ufl.edu (K.R. Gurley).
[1] Tel.: +1-352-392-9537x1508; fax: +1-352-392-3394.

0045-7949/03/$ - see front matter
doi:10.1016/S0045-7949(03)00058-0

2. Evaluation of a proposed work zone curb

A work zone curb is a temporary barrier system used to separate traffic from individuals working in roadside work areas. The study described herein began when the authors were asked by the Florida Department of Transportation (FDOT) to evaluate methods for fastening a proposed low profile work zone curb system to asphalt pavement [3]. The proposed system consisted of multiple concrete segments having a trapezoidal cross-section and a vertical height of approximately 230 mm (9 in.). A thin coat of sprayed asphalt (i.e. a "tack-coat") was going to be used to adhere the curb segments to the roadway surface. The goal was to quantify the shear strength requirements of the tack-coat. Impact conditions, for which the curb system was to perform adequately, were designated by the FDOT as a 2050 kg (4500 lbf) pickup truck striking the curb at 72 km/h (45 miles/h) at an angle of 15°. If the tack-coat fastening method proved to have insufficient strength, then a supplementary attachment system would be developed to provide the required bond strength.

The low profile of the proposed curb system presented a set of potential problems not anticipated by the FDOT in the problem statement. Even if a fastening system could be developed that possessed sufficient strength, it would do little good if vehicles were able to cross the curb during impacts and enter the work zone. To investigate this possibility, multiple numeric simulations were conducted using two independent computer simulation programs to study the behavior of pickup trucks impacting the proposed curb. Initially, the highway vehicle object simulation model (HVOSM) [4] software was used to simulate a typical Chevy C20 pickup truck impacting the curb at various speeds and angles. The HVOSM simulations predicted that the proposed 230 mm (9 in.) curb shape would not be able to reliably redirect an errant pickup truck away from the work zone even if the curb-to-roadway bond was infinitely strong.

This conclusion was further corroborated through simulations conducted using the impact finite element code LS-DYNA. Using a modified version of a public domain finite element model of a Chevy C2500 pickup truck (discussed in further detail later in this paper), the HVOSM results were confirmed by LS-DYNA simulations. Based on these results, the focus of the research effort was redefined. The new focus was to develop a portable concrete work zone barrier that could meet the following criteria:

- *Crash test validation*: System must meet the NCHRP 350 [1] Level 2 requirements for longitudinal barriers. This requires full scale crash tests at 72 km/h (45 miles/h) for both a small car (820 kg, 1800 lbf, 20 degree impact angle) and a standard pickup truck (2000 kg, 4400 lbf, 25 degree impact angle).
- *Portable and modular*: System must be composed of easily movable units that can be assembled in the field and modularly replaced as necessary (e.g. after an impact).
- *Low profile*: System must have a low profile (short height) to allow drivers unhindered visibility of pedestrian and vehicle cross traffic.
- *Minimal anchorage*: Performance of the system should not be highly dependent on anchorage of the barrier to existing pavement.
- *Minimal work zone intrusion*: System should allow minimal lateral barrier deflection into the work zone during an impact and redirect vehicles away from the work zone.

In order to design a barrier system that could achieve these goals with minimal crash testing costs, extensive use was made of the finite element simulation code LS-DYNA.

3. Finite element modeling techniques

For a longitudinal work zone barrier to be acceptable, it must be capable of smoothly redirecting errant vehicles of various sizes away from the work area being protected. NCHRP 350 requires crash tests be conducted using both a 2000P vehicle (a 2000 kg pickup truck) and an 820C vehicle (an 820 kg compact car). The 2000P vehicle delivers more energy on impact than does the 820C and has a higher center of gravity making it more prone to rollover. As a result, primary focus in this research effort was placed on designing a new barrier system to successfully resist impact by a 2000P truck. It was assumed (correctly as will be demonstrated later) that if the barrier could pass physical crash testing with a 2000P truck, it would also pass testing with an 820C car.

3.1. Suspension modifications made to the NCAC C2500 finite element model

Since the Chevy C2500 pickup truck is the most common vehicle used in 2000P crash testing, extensive use of a finite element model of a C2500 truck was used in this research. The National Crash Analysis Center (NCAC) has developed a number of finite element models for common test vehicles and has released these models into the public domain. The model used in this research was a modified version of the NCAC Chevy C2500 reduced resolution (version 8) pickup truck model [5]. The original C2500 model developed by NCAC has a great deal of merit and has been widely and successfully used by the roadside safety community for

several years. However, in the course of conducting curb and barrier impact simulations, the authors have identified some aspects of the model that required modification for this application. These changes enhance the applicability of the model to impacts involving significant deformation of the front suspension springs.

Specifically, in the original NCAC model the stiffness of the front suspension coil springs was too small, pre-compression forces in the springs (needed to account for gravity loading) were not present, and the specifications of contact surface definitions in the vicinity of the front suspension control-arms were in need of improvement [3,6]. These aspects of the model do not present themselves in impact conditions where the front suspension deformations are not of great significance. For example, in frontal or oblique impacts on tall vertical rigid walls, vehicle response is affected by structural deformation of the vehicle body more than by compression and rebound of the suspension springs. However, for low profile barriers and curbs, the deformation of the suspension springs is important in determining redirection and trajectory of the vehicle both during and after impact.

Shown in Fig. 1 are two views of the front wheel and suspension assembly of the reduced resolution C2500 truck model. Each front suspension assembly is composed of two control-arms: upper and lower rotating control-arms. Discrete spring and damper elements connect the two control-arms together to simulate the effects of automotive coil springs and shock absorbers. Spherical joints connect the control-arms to the knuckle of the wheel assembly and revolute joints connect the arms indirectly to the chassis rail (allowing the arms to rotate about the axes of the revolute joints). In the NCAC model, the discrete spring elements have a stiffness of 14.4 N/mm (82.2 lbf/in.) and zero initial pre-compression (i.e., no initial "spring offset").

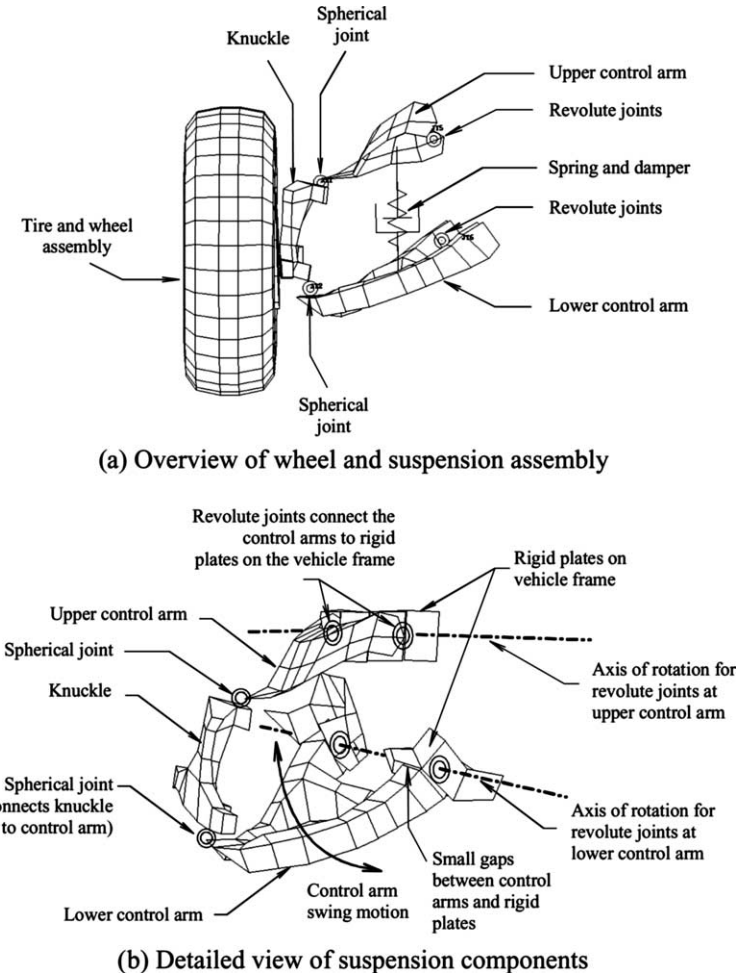

Fig. 1. Front wheel and suspension assembly of the NCAC C2500 model.

Under normal static gravity loading, the front suspension *springs* (not the tires) of a C2500 pickup truck will carry approximately 7750 N (1742 lbf) of force. For the stiffness specified, this would require 538 mm (21.2 in.) of spring deformation to reach equilibrium with gravity loading. The reason that analysts using this NCAC model generally do not observe such large spring deformations under combined gravity and impact loading is revealed in Fig. 2. The control-arms are attached to rigid plates through the revolute joints previously mentioned. These rigid plates are then attached to the deformable chassis rail of the pickup. However, there is only a very small clearance between the control-arms and the rigid plates. As soon as gravity is applied and the arms attempt to rotate upward, they immediately come into contact with the rigid plates (Fig. 2a) thus stopping the upward arm motion and preventing the discrete spring elements from being deformed. The vehicle comes into equilibrium with gravity not by correctly compressing the springs, but by resting on the rigid plates. This is an acceptable condition for some types of impact conditions because the center of gravity

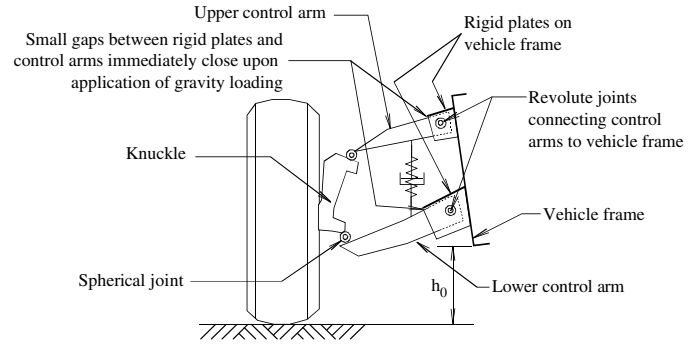

(a) Response of flawed suspension model under gravity loading

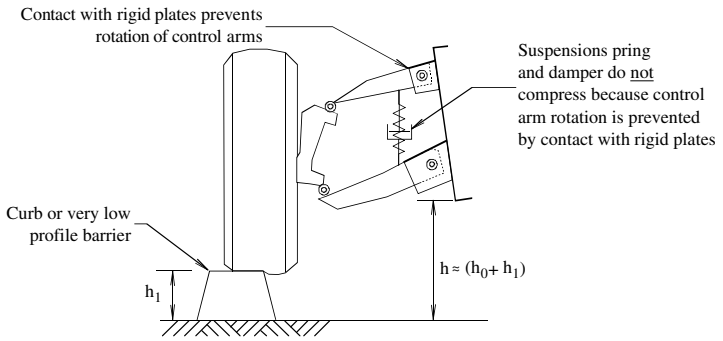

(b) Response of flawed suspension model under impact loading

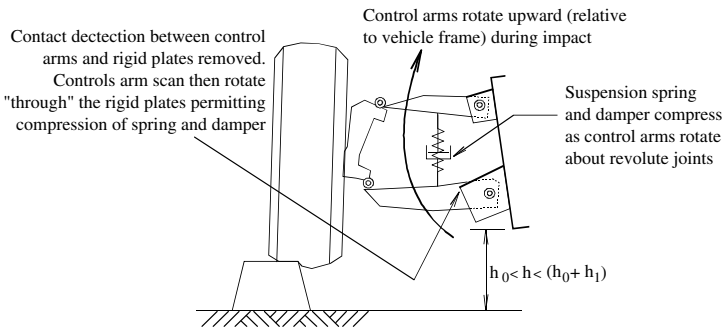

(c) Response of corrected suspension model under impact loading

Fig. 2. Rigid plates prevent rotation of front suspension control-arms.

(CG) of the vehicle is at the correct elevation. In many situations, the vertical position of the CG and deformation of the vehicle body (but not the wheels and suspension) are the primary factors affecting the outcome.

This modeling technique, however, is not appropriate for impact problems involving significant vertical movement of the front wheels (and thus compression and subsequent extension of the coil springs). For example, when a front wheel strikes a curb during an impact event, the suspension control-arms should rotate upward and compress the coil spring. It is clear that the original NCAC model was not intended for this type of application because the presence of the rigid plates prevents correct rotation of the control-arms (Fig. 2b). To enhance its applicability to impact conditions of this type, several modifications were made to the NCAC vehicle model. First, the contact definitions specified between the control-arms and the rigid plates were removed from the model. By removing these contact definitions, the control-arms can now pass "through" the rigid plates. Effectively, the rigid plates are now only used as a connection point for the revolute joints but no longer prevent rotation of the control-arms (Fig. 2c). Next, laboratory tests were conducted on typical C2500 coil springs to determine their actual stiffness. Results from the tests indicated that the load–deflection relationship for the coil springs was linear and that the linear stiffness was 166.5 N/mm (951 lbf/in.) [6].

Finally, the spring pre-compression required to balance gravity loading was determined. In the NCAC C2500 model, the position and orientation of the wheel and suspension components are modeled to match the *gravity-equilibrium configuration* of the vehicle. For example, the position of each front wheel relative to the vehicle body matches the position that the wheel would have if the truck were sitting at rest on a flat surface while subjected to standard gravitational body forces. In this configuration, the compressive force in each front suspension coil spring must be such that it produces the necessary equivalent force *at the centerline of the tire* so as to balance the reaction on the tire due to gravity loading. An initial discrete spring element "offset" (in LS-DYNA terminology) was used to produce the required initial spring compressive force. Using the laboratory measured spring stiffness, it was determined that an initial compressive offset (i.e. compressive spring deformation) of 46.5 mm (1.83 in.) was required to produce the spring force corresponding to the gravity-equilibrium position.

3.2. Frictional effects in finite element impact simulation

In addition to the suspension modifications described above, the authors also gave special attention to the representation of frictional effects. Frictional contact forces developed between tires and barrier contact surfaces can affect whether or not a particular barrier system will successfully redirect an impacting vehicle. Predictions of vehicle redirection obtained from finite element simulation are influenced by several factors—frictional effects, barrier impact face geometry, barrier stiffness, barrier inertial properties, finite element representations of vehicle components, and selection of contact algorithms. Among these factors, the representation of friction is often over simplified.

In the present study, individual contact and friction definitions were specified for steel-to-steel contact, steel-to-concrete contact, barrier-to-roadway contact, tire-to-roadway contact, tire-to-barrier contact, and barrier-to-barrier (i.e. concrete-to-concrete) contact. Particular attention was given to modeling friction between the vehicle tires and the barrier segments (tire-to-barrier contact). In general, the frictional force between two bodies in contact is determined based on the normal force and coefficient of friction (μ) that are active at the contact zone. The value of μ may be numerically modeled either as a fixed constant value or as a function of the velocity at which the surfaces slide past one another (v_{sliding}). Using the latter representation matches more closely with the velocity dependant nature of frictional development in materials such as vehicle tires. For example, when a rotating tire impacts a barrier at an oblique angle, different locations on the tire slide against the barrier at different velocities (especially in cases involving significant tire sidewall scrubbing). Thus, using a velocity dependent frictional model is most appropriate, although constant friction coefficients are often successfully used for cases involving very low profile systems (e.g. short curbs).

In the present study, experimental data obtained from the literature were used to develop velocity dependent friction models for representing tire-to-concrete contact. Yager et al. [7] reported test results for tire-to-concrete friction measurements and discussed the influence of parameters such as sliding speed, type and amount of surface contaminants, tire characteristics, and temperature. Their test data indicate that tire friction is sensitive to surface contamination, particularly for tire friction on dry concrete. Data presented by Gillespie [8] further corroborate sensitivity to surface condition. Friction is also affected by tire properties such as tread pattern and hardness [9], roughness of the roadway surface (e.g. concrete texture) and tire wear [10].

Given this variability, the approach taken in this study was to bracket the expected range of frictional values with upper and lower bound limits and then to run simulations at each of these limits to evaluate system performance. If a constant friction model is being used (rather than a velocity dependant friction model) then establishing upper and lower bound friction models

simply amounts to choosing scalar upper and lower bound values. For the barrier being developed in this study, however, it was anticipated that during vehicle impacts, significant scrubbing contact would occur between the vehicle tires and the barrier. For this reason, a velocity dependent friction model was deemed to be more appropriate than a constant friction model. Using data for tire-to-concrete friction obtained from the references cited above and accounting for the typical characteristics of roadside work zones, upper and lower bound friction curves were established for use in designing the barrier system that was the focus of this study. The functional form of these curves is given by

$$\mu = \alpha + \beta e^{-\gamma(v_{\text{sliding}})} \tag{1}$$

where α, β, and γ are fitting parameters chosen to produce the desired velocity dependency of the friction coefficient. The upper bound curve, μ_{upper}, and lower bound curve, μ_{lower}, used to design the barrier discussed herein are graphically illustrated in Fig. 3. In addition, a *very* low friction curve $\mu_{0.2\times\text{lower}}$ (the lower bound design curve multiplied by 0.2) is also shown in the figure. This last curve does not represent realistic tire-to-barrier friction but is used herein to illustrate various numerical simulation issues.

Recognizing that the fundamental role of a longitudinal barrier is to *redirect* errant vehicles, consider the following example which illustrates the influence that friction can have on simulation predictions. A 2000P vehicle impacts a 225 mm (9 in.) work zone curb at a 15 degree impact angle. Two simulations are performed: one in which tire-to-curb friction is represented using the upper bound design friction curve $\mu = \mu_{\text{upper}}$ and a second case in which the very low friction model $\mu = \mu_{0.2\times\text{lower}}$ is used. In both cases, the bond between the curb and the roadway is assumed to be perfect, i.e. the curb itself does not slide. Predicted vehicle trajectories for both cases are illustrated in Fig. 4. The first case ($\mu = \mu_{\text{upper}}$) predicts that the vehicle over-rides the curb—a condition that is unacceptable if the curb is intended to protect the work zone. In contrast, the reduced friction in the second case ($\mu = \mu_{0.2\times\text{lower}}$) prevents the vehicle tires from climbing the curb, and instead successful redirection of the vehicle is predicted. This example clearly points out that the magnitude of friction introduced into a simulation—whether introduced through the use of a constant friction model or a velocity dependent friction model—can significantly alter the predicted results. Conducting separate impact simulations for a system using appropriately chosen upper and lower bound friction models can help ensure that the full range of post-impact outcomes has been considered.

Fig. 5 expands on this example by illustrating the kinetic and internal strain energy histories corresponding to the two simulations cited above. It is evident that more energy is dissipated in the case where a higher level of friction is introduced (i.e. μ_{upper} in Fig. 3). In this case, the kinetic energy drops much faster than the internal strain energy rises—the difference in the two being primarily attributable to energy dissipated by frictional

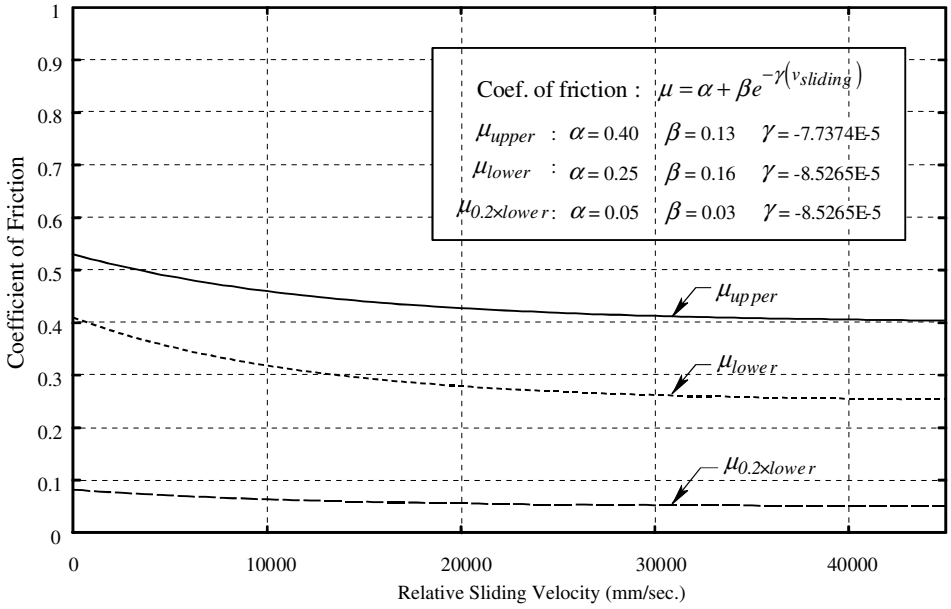

Fig. 3. Frictional relationships for tire-to-barrier contact.

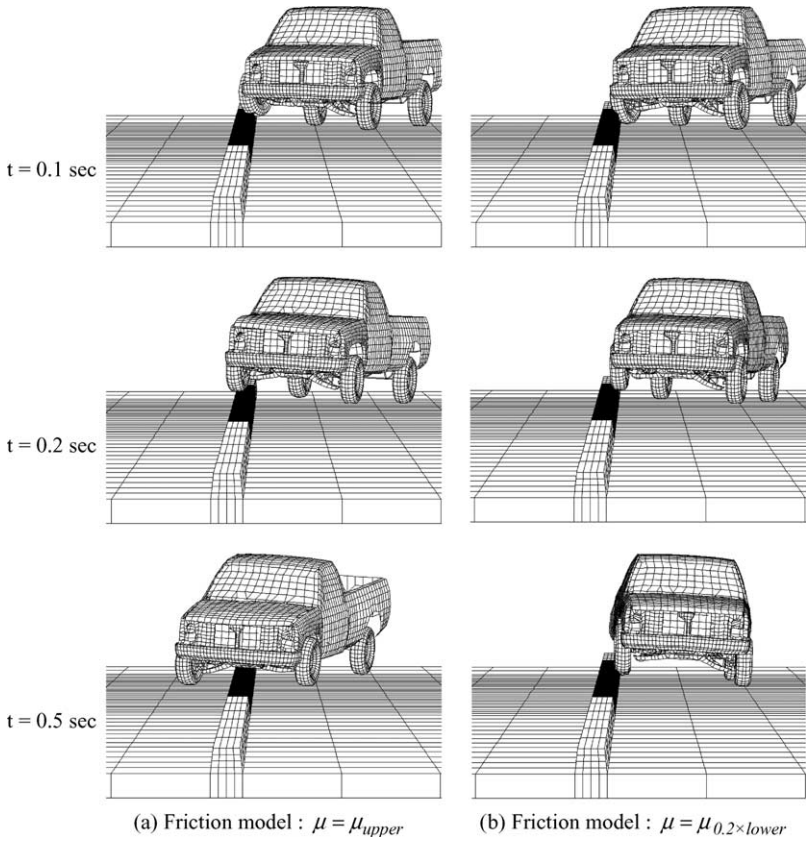

Fig. 4. Curb impact simulation results for different frictional models.

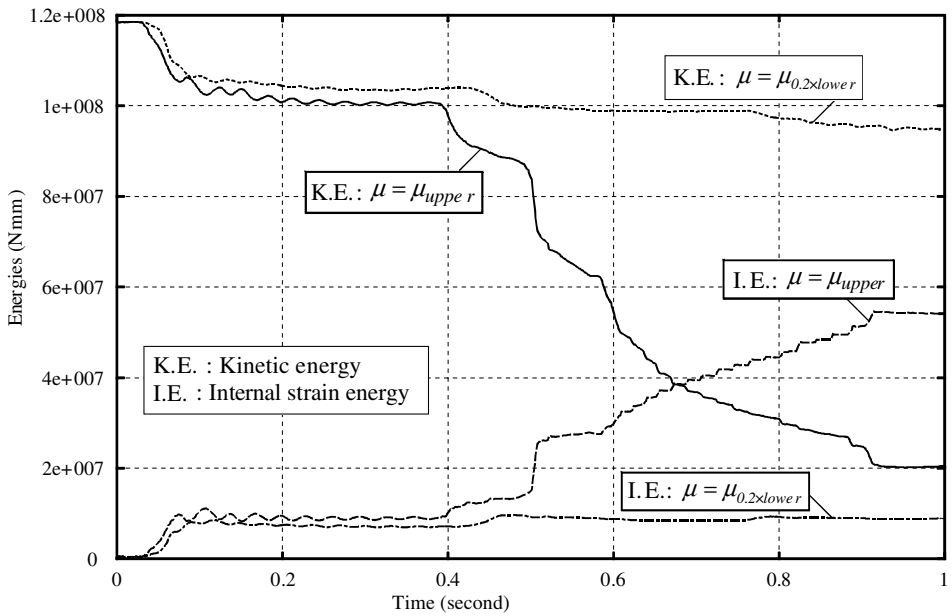

Fig. 5. Kinetic and internal system energies for curb impact simulations.

forces. In contrast, the case where $\mu = \mu_{0.2\times\text{lower}}$ indicates only a moderate drop in kinetic energy and less energy dissipation. Accounting for such dissipation is an important element of designing roadside barrier systems using simulation because predicted measures of vehicle behavior (e.g. maximum roll angle and exit angle) are directly influenced by the degree of energy dissipation occurring during the impact. Additionally, in the case of concrete barrier systems made up of individual segments joined together via connection bolts, the peak forces experienced by the bolts will vary significantly with changes in dissipated energy.

4. Energy monitoring as a means of improving simulation reliability

Examining the balance of system energy components—kinetic, potential, dissipated, etc.—during a simulation can be helpful in identifying the predominant factors affecting vehicle or barrier response during an impact. In addition, monitoring energy components also serves as a key step in identifying the presence and causes of numerical instabilities that may arise in explicit dynamic finite element impact simulation.

Interpreting energy balance information is most easily accomplished by first considering the principle of the conservation of energy for a physical system. At any given instant in time, t, the total mechanical energy (E) of a system can be expressed as

$$E = T + W \tag{2}$$

where T is the kinetic energy and W is the potential energy. Furthermore, W can be split into internal strain energy and external work done denoted by W^{internal} and W^{external} respectively:

$$E = T + W^{\text{internal}} - W^{\text{external}} \tag{3}$$

If all of the forces acting on a system are purely conservative, then Eq. (3) states that the balance of kinetic energy, internal strain energy, and external work done is conserved at all points in time. The law of conservation of mechanical energy then states that the total mechanical energy of the system (E) is constant with respect to time and changes in kinetic energy (T) are balanced by changes in potential energy (W) as follows:

$$\Delta T + \Delta W = \Delta T + \Delta W^{\text{internal}} + \Delta W^{\text{external}} = 0 \tag{4}$$

In real physical systems, however, non-conservative forces often play an important role and cannot be neglected. Irreversible processes such as plastic deformation of mechanical components and frictional sliding at contact interfaces dissipate energy in a non-conservative manner. To account for the reduction in mechanical system energy associated with the effects of non-conservative forces, a dissipation term must be added to the conservation of energy equation:

$$\Delta T + \Delta W^{\text{internal}} + \Delta W^{\text{external}} + \Delta U^{\text{dissipation}} = 0 \tag{5}$$

where ΔT represents the change of kinetic energy occurring over some increment of time, $\Delta W^{\text{internal}}$ represents the change of internal (strain) energy, $\Delta W^{\text{external}}$ is the external work done, and $\Delta U^{\text{dissipation}}$ represents energy dissipated by frictional forces, plastic deformation, and system damping (e.g. vehicle suspension damping).

Summing all energy, work, and dissipation terms for the physical system at time t and normalizing with respect to the total mechanical energy (E), we have

$$\frac{T + W^{\text{internal}} - W^{\text{external}} + U^{\text{dissipation}}}{E} = 1 \tag{6}$$

where W^{external} represents total work done, $U^{\text{dissipation}}$ the total energy dissipated, T the kinetic energy, W^{internal} the internal strain energy, and E the total mechanical energy of the system. However, in terms of writing an energy balance expression for a numerical *model* of a physical system, certain non-physical energy terms will need to be added to Eq. (6). Of particular interest in LS-DYNA simulations is an hourglass energy term that relates to unstable deformation modes that can occur when using under-integrated finite elements.

Due to their computational efficiency, under-integrated (reduced integration) element formulations—some using as few as a single numeric integration point per element—are often used for both solid and shell elements in LS-DYNA simulations. Given that explicit dynamic analysis typically requires very small time step sizes in order to preserve solution stability, minimizing the computational effort involved in each time step by using reduced element integration is very attractive. However, while such an approach is highly efficient from a computational standpoint, it is well known that under-integrated formulations frequently lead to the development of spurious zero energy (hourglass) modes Ref. [11, Section 5.5.5]. Element hourglassing often arises in localized zones of a model as the dynamic time-stepping process progresses. Left uncontrolled, the size of these zones and severity of the hourglassing can increase until the entire model is rendered unstable and the simulation terminates.

In developing large-scale LS-DYNA simulation models, analysts often choose to represent critical portions of a system (contact zones, areas in severe deformation, etc.) using fully integrated elements, which do not suffer from hourglassing, and the remaining portions using under-integrated elements. Hourglass control algorithms may then be activated for elements in the under-integrated portions of the mesh. Through a variety of different techniques [2], these algorithms *attempt*

to suppress the development and spread of hourglass deformation patterns in the model. When successful, hourglass control permits the use of computationally efficient under-integrated elements in situations where fully integrated elements would normally be required to prevent model instabilities from occurring. However, use of these algorithms does not guarantee that hourglass deformation will not occur.

Therefore, simulations utilizing under-integrated elements must be carefully monitored if reliable results are to be obtained (regardless of whether hourglass control is used or not). When hourglass instabilities occur, they often grow sufficiently large so as to be detectable by simple visual inspection of simulation results. However, subtle instabilities can also occur that while not presenting themselves visually can nevertheless affect the results obtained. Consider Fig. 6 in which results are presented for simulated vehicle impacts on 9-inch concrete curbs using two different tire-to-curb friction models: $\mu = \mu_{\text{upper}}$ and $\mu = \mu_{0.2\times\text{lower}}$. Impact conditions and system modeling for the simulations shown in Fig. 6 were virtually identical to those used to generate Fig. 4 (discussed earlier). In both sets of cases (Figs. 4 and 6), the vehicle models consisted of a mixture of both fully integrated elements and under-integrated elements. The sole difference between Figs. 4 and 6 was in the shell element formulation used to model selected portions of the impacting vehicle. Fully integrated shell elements were used in several areas of the vehicle model—front bumper, cabin, fender panels, frame, front tires and rims—corresponding to Fig. 4 while under-integrated shell elements without hourglass control were used throughout the entire vehicle model corresponding to Fig. 6.

In Fig. 6a, severe hourglass deformation occurs immediately upon impact and is followed by vehicle behavior that, upon visual examination, is clearly non-physical in nature and therefore suspect. All simulation results following the initial hourglass instability are considered to be error-polluted and therefore not reliable. In contrast, Fig. 6b presents a less obvious situation. Despite the very low coefficient of friction used ($\mu = \mu_{0.2\times\text{lower}}$), results indicate that the vehicle overrides the curb. Visual inspection of the simulated vehicle behavior at several points in time does not reveal any apparent anomalies. However, the predicted outcome—i.e., non-redirection of the vehicle during impact—is quite different from that obtained earlier in Fig. 4b where the vehicle *was* redirected.

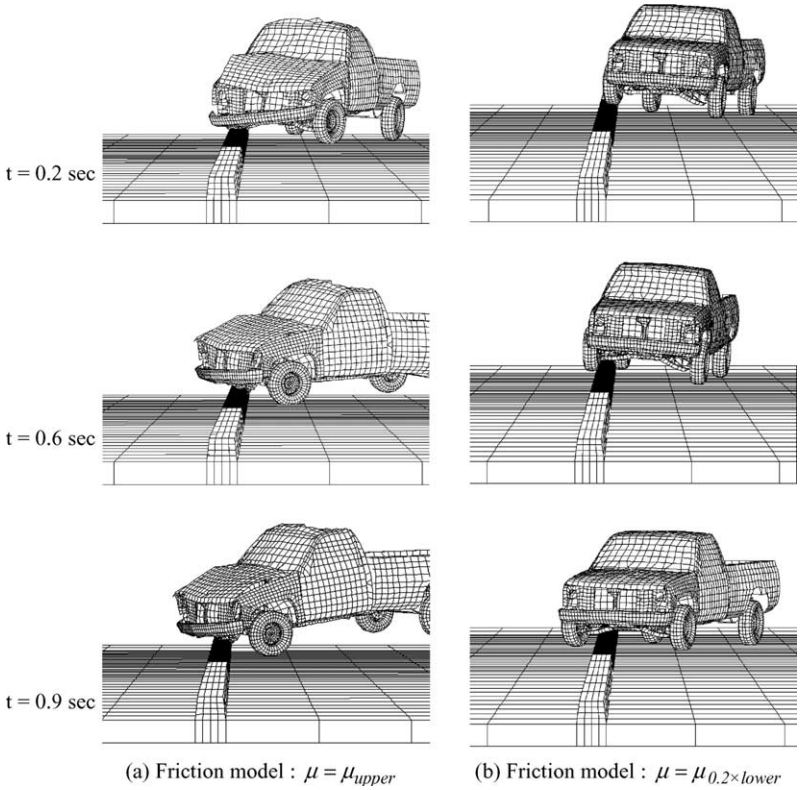

Fig. 6. Curb simulations conducted using under-integrated shell elements.

In order to determine which prediction is more reliable—Fig. 4b or Fig. 6b—we return to the concept of a normalized energy ratio as given by Eq. (6). Although not performed by default, LS-DYNA can be instructed to compute and include in the system energy balance the energy ($E^{\text{hourglass}}$) associated with solid and shell elements undergoing hourglass modes of deformation. Since hourglassing is a purely numerical occurrence having no corresponding physical phenomenon, it is important that the size of the hourglass energy term remain very small relative to the overall system energy throughout a simulation. If hourglass energy becomes a significant portion of the overall system energy balance, this is an indication that non-physical phenomena are unduly influencing the simulation. In such situations, the results should be regarded as potentially unreliable.

Quantifying the amount of hourglass energy thus provides a useful tool for determining whether a simulation has been polluted by artificial numerical effects. In this study, the ratio of the hourglass energy to total mechanical system energy was used for this purpose. If the normalized hourglass energy ($\overline{E}^{\text{hourglass}}$) remains negligibly small:

$$\overline{E}^{\text{hourglass}} = \frac{E^{\text{hourglass}}}{E} \approx 0 \tag{7}$$

then it is very probable that the simulation results are free of serious hourglassing effects. While Eq. (7) is a necessary condition for gaining confidence in a simulation model, it is not sufficient to guarantee that accurate results have been obtained. Developing an adequate level of confidence in the robustness of a model typically requires completion of additional steps—e.g. conducting parameter sensitivity studies, studying the physical response of the model, conducting mesh convergence studies, and performing component-level or system-level physical validation testing (whenever feasible). However, if Eq. (7) is *not* satisfied, then pursuing these additional steps is premature since the presence of non-negligible hourglass energy is an indication of potential model deficiencies.

In Fig. 7 the quantity $\overline{E}^{\text{hourglass}}$ is plotted for the simulation examples described above. Results from "FI" cases (fully integrated elements used in portions of the vehicle model) are compared to "UI" cases (under-integrated elements used throughout the vehicle). The results confirm what was not obvious from simple visual inspection—namely that Fig. 4b represents a more reliable prediction of the impact outcome than does Fig. 6b. The $\overline{E}^{\text{hourglass}}$ curve for case FI-b (selective use of fully integrated elements, $\mu = \mu_{0.2\times\text{lower}}$, Fig. 4b) remained acceptably small throughout the entire simulation. The small amount of hourglass energy still present in the FI-b case corresponded to negligible hourglassing of under-integrated portions of the vehicle model, not to the fully integrated portions. In contrast, the $\overline{E}^{\text{hourglass}}$ curve for case UI-b (under-integrated, $\mu = \mu_{0.2\times\text{lower}}$, Fig. 6b) ex-

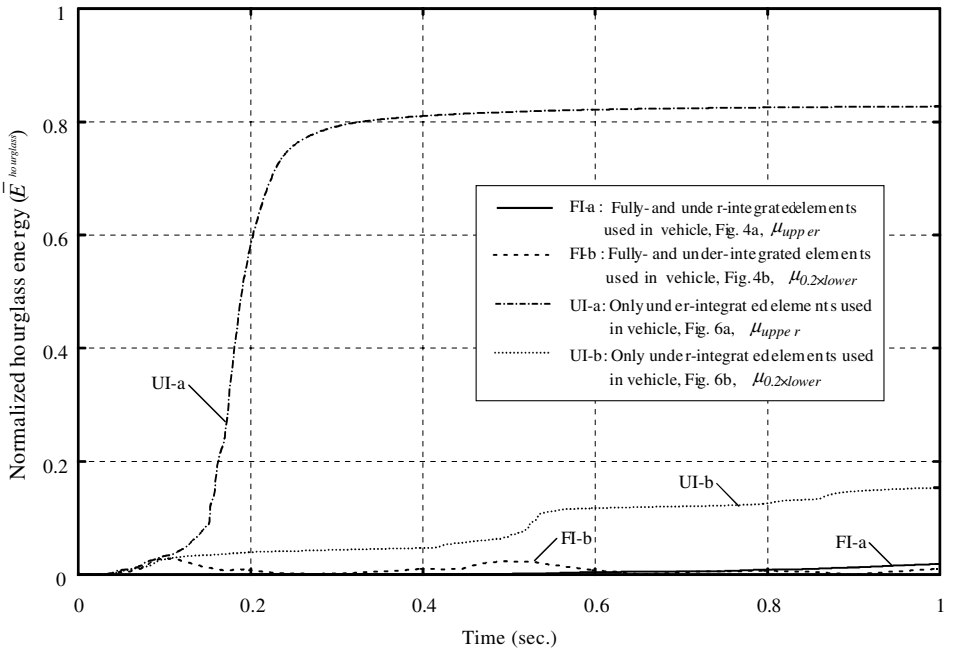

Fig. 7. Normalized hourglass energy for curb impact simulations.

ceeded 10% at approximately $t = 0.6$ s and continued growing throughout the simulation. This trend indicated significant hourglass pollution of the results despite the fact that anomalies were not obvious by visual inspection. By monitoring $\overline{E}^{\text{hourglass}}$, it was clear that hourglassing effects were non-negligible and thus any predictions from the simulation were questionable.

For comparison, Fig. 7 also includes plot of $\overline{E}^{\text{hourglass}}$ for the FI-a (fully integrated, $\mu = \mu_{\text{upper}}$, Fig. 4a) and UI-a (under-integrated, $\mu = \mu_{\text{upper}}$, Fig. 6a) cases. In case FI-a, $\overline{E}^{\text{hourglass}}$ remained less than a few percent throughout the entire simulation as in the FI-b case. Thus, neither FI-a nor FI-b had significant hourglass pollution. In contrast, $\overline{E}^{\text{hourglass}}$ increased rapidly in the UI-a case which is consistent with the non-physical behavior visually evident in Fig. 6a. Therefore, monitoring hourglass energy during vehicle impact simulations should be considered an essential element in ensuring that reliable results are obtained. If $\overline{E}^{\text{hourglass}}$ grows to an unacceptably large level—based on the experience and judgment of the analyst—then the simulation results should be considered unreliable.

5. New barrier development using finite element analysis impact simulation

Using the modified C2500 model, the new friction relationships, and the energy monitoring processes described above, the authors began the process of developing a new low profile portable concrete barrier system that would meet the design criteria previously outlined. Each cycle of the iterative development process consisted of a concept development followed by extensive computer simulations of the proposed design.

Prior to starting the development process in full, a literature review was conducted to determine if any presently available barrier system would satisfy the required design criteria. Of all the systems reviewed, the segmental concrete barrier shape reported by Guidry and Beason [12] was given the most serious consideration as it was reported to have performed well in crash tests involving pickup truck impacts. It was also moderately portable in the sense that it consisted of segments that were joined together using field-installed connection bolts. However, the weight and length of each segment were sufficiently large so as to preclude the use of smaller pieces of construction equipment (e.g. light weight forklifts, etc.) for field installation and removal procedures. The authors believed that a new system could be developed that would provide comparable redirectional performance using significantly lighter and shorter segments. After reviewing several other systems, it was concluded that no currently available barrier system would meet all of the design criteria specified. Development of a new system was thus undertaken.

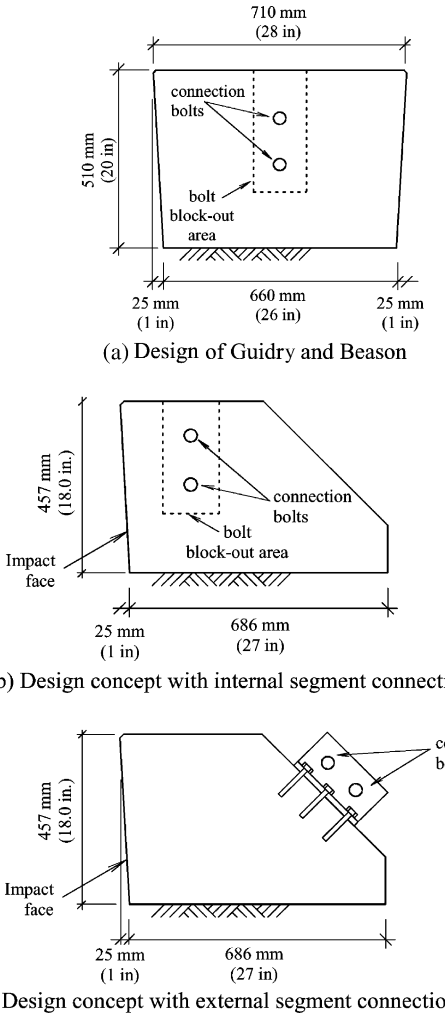

(a) Design of Guidry and Beason

(b) Design concept with internal segment connection bolts

(c) Design concept with external segment connection brackets

Fig. 8. Barrier design concepts considered.

The first concept developed consisted of concrete segments similar to but lighter and shorter than those of Guidry and Beason. Their system consists of segments that were 508 mm (20 in.) tall, 6.1 m (20 ft) long, had an inverted trapezoidal cross-sectional shape (see Fig. 8), and weighed 49 kN (11 kips) each. The first concept developed by the authors used segments that were 457 mm (18 in.) tall, 3.7 m (12 ft) long, had a truncated slanted triangular cross-section (see Fig. 8b), and weighed only 21 kN (4.6 kips) each. Computer simulations conducted for the new system indicated suitable redirectional capability when impacted at 72 km/h (45 miles/h) and 25° by a 2000P vehicle. Initially the new design called for connection bolts installed through "blocked out" sections at the ends of the barrier segments. However, after

building prototype formwork for this design, it was concluded that there was excessive congestion of reinforcing steel and that a new connection method was needed.

A new connection detail in which external brackets were attached to the back (sloping) faces of the segments was then explored (see Fig. 8c). By running connection bolts through external brackets on each set of adjacent barrier segments, the bolt block-outs were eliminated and the reinforcing cage was simplified. However, subsequent simulations revealed a serious flaw in this design—the bolts spanning between the brackets did not transfer adequate shear force. As a result, during an impact the barrier segments displaced relative to one another sufficiently to create snagging points. Fig. 9 shows a simulation in which portions of the vehicle cabin snag on protruding downstream barrier segments. The vehicle undergoes a harsh deceleration (resulting in a rapid decrease in longitudinal velocity between $t = 0.32$ and 0.38 s) and virtually comes to a stop before finally separating from the snag point. Due to the potential for this type of snagging, this design concept was abandoned.

Eventually a final design evolved in which the connection bolts were still near the back face of the barrier but were now embedded in the concrete cross-section. Fig. 10 presents both detailed design drawings and photographs of the system. A load transfer assembly was designed that takes the load from the connection bolt and transfers it to the concrete via shear studs and additional embedded bolt length. This connection design is capable of carrying the tensile loads in the bolts but is also able to transfer shear from one segment to the next during impact, thus eliminating the snagging problem. In addition, the connection bolts provide stiffness and flexural continuity during impact so that several segments near the impact location are mobilized. The collective flexural and inertial resistances of the mobilized segments are sufficient to redirect an errant vehicle and anchorage of the barrier system to the existing pavement is unnecessary, greatly simplifying field installation of the system.

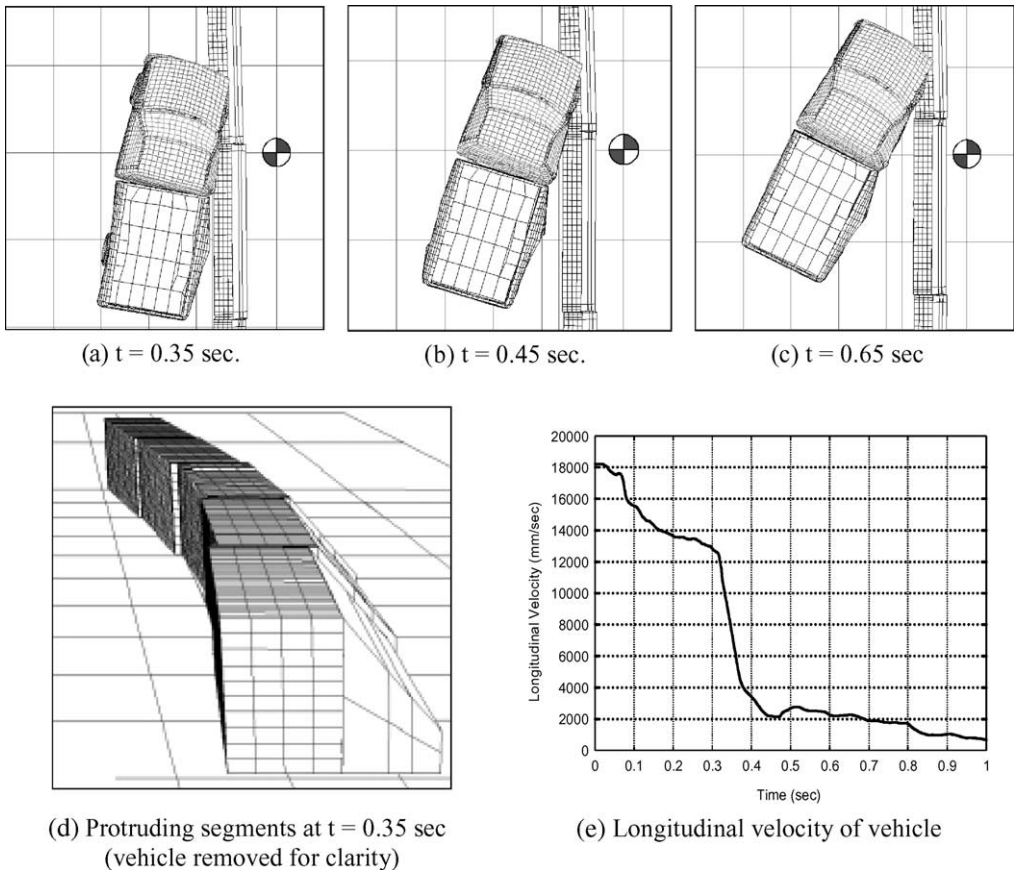

Fig. 9. Vehicle snagging due to relative sliding motion between barrier segments for connection system shown in Fig. 8c.

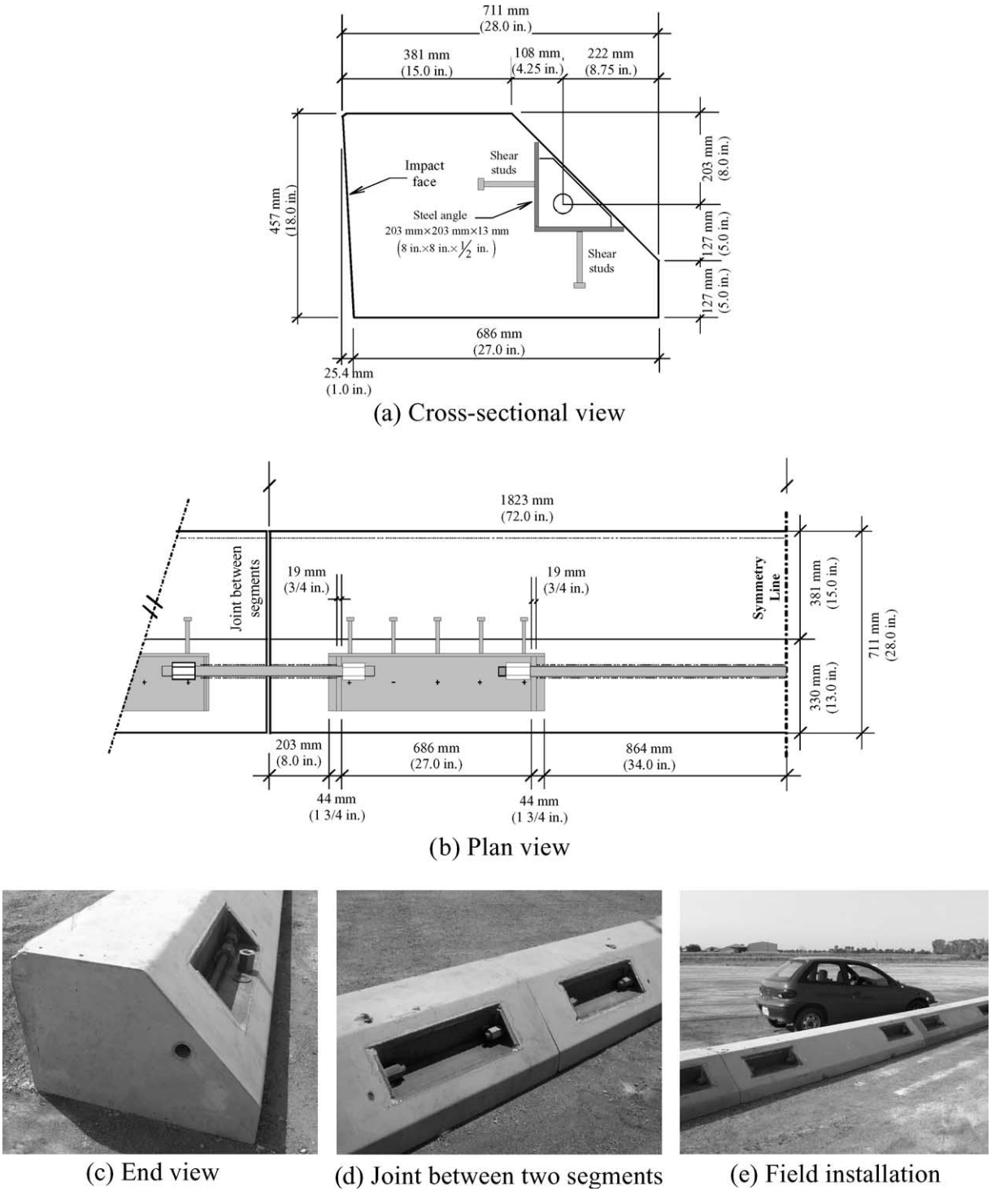

Fig. 10. Final barrier design.

A comprehensive series of impact simulations were performed using the final design concept in an attempt to ensure success during full scale crash testing. Simulations were performed using both the upper and lower

bound friction curves of Fig. 3 to evaluate the redirectional capability of the barrier and to determine the critical design forces for the connection bolts and load transfer assemblies.

6. Full scale validation and crash testing

In order to validate the field performance of the proposed system, which was developed based purely on finite element simulations, two full scale crash tests were performed. As recommended by NCHRP 350, the barrier assembly was impact tested using both an 820C compact car and a 2000P pickup truck. Ten barrier segments were fabricated and connected together to form a test article that was 36.6 m (120 ft) in length. This choice of system length was fully justified by the test results as the segments at both ends of the system did not displace at all during either the 820C or 2000P impact tests. The impact tests were conducted at the facilities of E-Tech Testing Services located in Rocklin, CA, USA.

Results from the full scale tests are shown in Table 1. In both tests, the test vehicle exited the barrier at a very small angle and with minimal damage to the vehicle (both vehicles sustained a single suspension joint failure during impact). Lateral deflection of the barrier into a hypothetical work zone located behind the system was less than 191 mm (7.5 in.) despite the fact that the barrier was not anchored to the roadway. Frictional resistance between the bottom of the barrier and the roadway at the test site represented worst case conditions as the roadway surface consisted primarily of loose chipped asphalt with a low coefficient of friction. Occupant risk measures for both tests were within allowable limits. Even with its low profile, the barrier was able to redirect the 2000P vehicle without the occurrence of rollover, barrier connection failure, or snagging.

Fig. 11 shows a comparison of crash test results and simulation results (for $\mu = \mu_{\text{upper}}$) for the 2000P impact condition. The two sets of results are generally in good agreement with the overall vehicle motions matching reasonably well and the exit angles being very similar. The most notable differences are in the behavior of the front tire during impact and the maximum roll angle sustained. In the simulation, the front impact tire steers more excessively than in the crash test resulting in a longer duration of contact between the tire and the barrier. As a result, more kinetic energy is dissipated through friction in the simulation and a smaller maximum roll angle is predicted. The steering angle discrepancy is believed to be caused by the properties of the steering control mechanism present in the model and is being investigated. Lateral barrier deflections predicted by the upper and lower bound simulations bracket the crash test results closely, and justify the methodology of system design based on simulation followed by crash test validation.

7. Conclusions

By making extensive use of finite element impact simulation, a new low-profile portable work zone barrier system has been successfully developed and tested. Several cycles of conceptual design refinement were

Table 1
Summary of crash test results and simulation results

Test parameter	820C Test (Geo Metro car)	2000P Test (Chevy C2500 pickup)	2000P Simulation (upper bound friction)	2000P Simulation (lower bound friction)
Impact speed	70.6 km/h (44 miles/h)	68.0 km/h (42.3 miles/h)	68.0 km/h (42.3 miles/h)	68.0 km/h (42.3 miles/h)
Impact angle	20°	25°	25°	25°
Vehicle exit speed	48.6 km/h (30.2 miles/h)	43.6 km/h (27.1 miles/h)	42.3 km/h (26.3 miles/h)	44.3 km/h (27.5 miles/h)
Vehicle exit angle	5°	0°	3.0°	2.5°
Dynamic deflection	64 mm (2.5 in.)	190 mm (7.5 in.)	174 mm (6.9 in.)	327 mm (12.9 in.)
Permanent deflection	51 mm (2.0 in.)	165 mm (6.5 in.)	157 mm (6.2 in.)	280 mm (11.0 in.)
Maximum roll angle	−4.3°	29.7°	7.0°	8.4°
Maximum pitch angle	−6.2°	−12.1°	−1.1°	−1.3°
Maximum yaw angle	−58.6°	−25.1°	−27.5°	−29.1°
Occupant longitudinal ridedown acceleration	−3.6*g*	−3.7*g*	(Not computed for simulations)	
Occupant lateral ridedown acceleration	−10.6*g*	−6.3*g*		
Occupant longitudinal impact velocity	3.6 m/s (11.8 ft/s)	4.0 m/s (13.1 ft/s)		
Occupant lateral impact velocity	−4.3 m/s (−14.1 ft/s)	−3.7 m/s (−12.1 ft/s)		

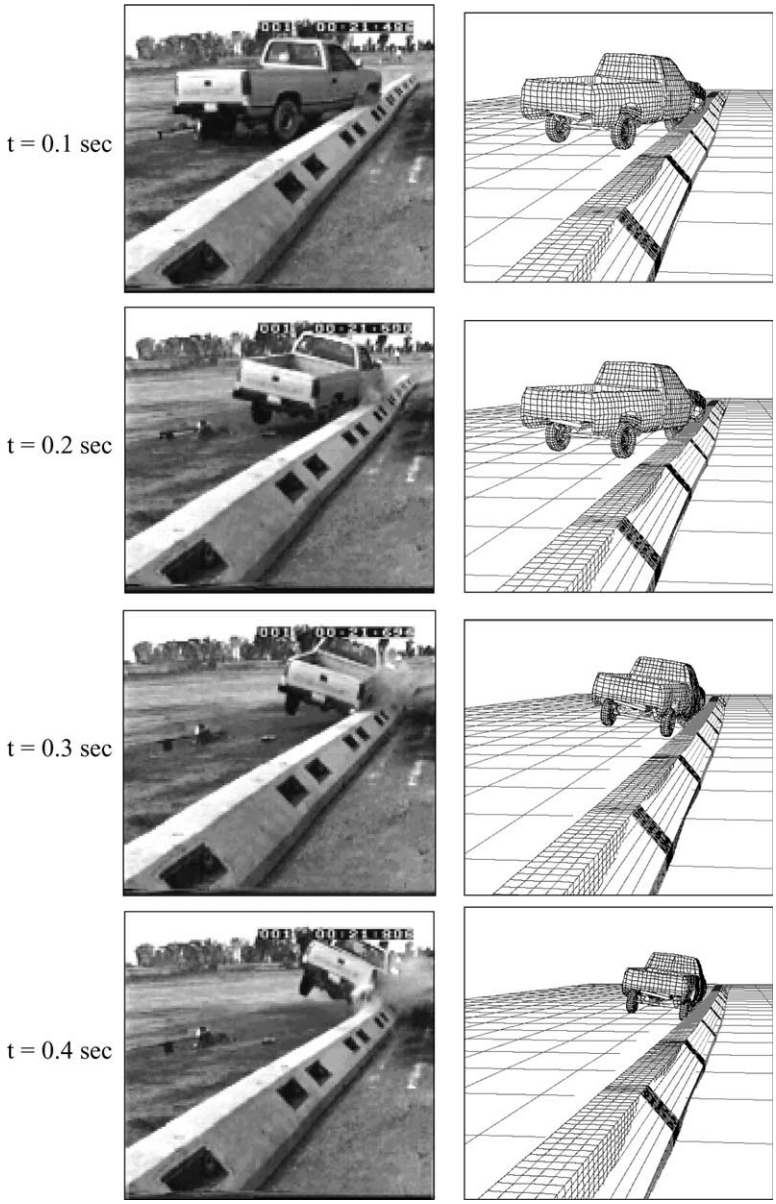

Fig. 11. Comparison of crash test results and simulation results for 2000P vehicle.

performed based purely on computational simulation thus substantially reducing both the time and costs associated with development of the system. Modifications to the NCAC C2500 reduced resolution pickup truck model have been made to expand its applicability to impact conditions involving significant deformation of the front suspension assemblies.

The influence of frictional effects between vehicle tires and concrete curbs and barriers has been demonstrated through numeric examples. Upper and lower bound velocity dependant frictional relationships for such cases have been proposed. Energy balance issues have been discussed and the importance of monitoring hourglass energy variations during simulations involving under-integrated finite elements has been demonstrated through numeric examples. It is recommended that if the normalized hourglass energy in a system exceeds approximately 5% at any point during a simulation, the results should be considered unreliable and a revised system model should be developed.

Full scale crash tests involving both 2000P and 820C vehicles were successfully carried out and good

agreement between the 2000P simulation results and crash test results were observed. Despite its low profile, the barrier was able to successfully redirect even the 2000P vehicle without causing a rollover. Additionally, because the new barrier utilizes inertial resistance of multiple adjacent segments to redirect impacting vehicles, its performance does not require anchorage of the barrier segments to the roadway.

Acknowledgements

The authors wish to thank the Florida DOT for providing the financial support that made this research and development program possible. The material presented in this paper is based upon research that was supported by the FDOT under contract no. BB-894.

References

[1] NCHRP. Recommended procedures for the safety performance evaluation of highway features, Report no. 350, National Cooperative Highway Research Program, Transportation Research Board, 1993.
[2] Hallquist JO. LS-DYNA theoretical manual. Livermore, CA: Livermore Software Technology Corporation; 1998.
[3] Ellis R, Consolazio GR, Gurley KR, Chung JH. Investigation of improved procedures and technologies for managing the maintenance of traffic through FDOT work zones, University of Florida Structures Research Report no. 661-1, 2001.
[4] Segal DJ. Highway vehicle object simulation model (HVOSM), Report no. FHWA-RD-76-162, 1976.
[5] Zaouk AK, Bedewi NE, Kan CD, Marzougui D. Development and evaluation of a C-1500 pick-up truck model for roadside hardware impact simulation, FHWA/NHTSA National Crash Analysis Center, The George Washington University, 1997.
[6] Siridumrongphun A. Vehicle curb impact study using a nonlinear dynamic finite element simulation program, Master's thesis, Department of Civil & Coastal Engineering, University of Florida, 1999.
[7] Yager TJ, Vogler WA, Baldasare P. Evaluation of two transport aircraft and several ground test vehicle friction measurements obtained for various runway surface types and conditions: A summary of test results from joint FAA/NASA runway friction program, 1990.
[8] Gillespie TD. Fundamentals of vehicle dynamics. Society of Automotive Engineers 1992.
[9] Gunaratne M, Bandara N, Medzorian J, Chawla M, Ulrich P. Correlation of tire wear and friction to texture of concrete pavements. Journal of Materials in Civil Engineering 2000;12(1):46–54.
[10] Moore DF. The friction of pneumatic tires. New York: Elsevier Scientific Publishing Company; 1975.
[11] Bathe KJ. Finite element procedures. Englewood Cliffs, NJ: Prentice-Hall; 1996.
[12] Guidry TR, Beason WL. Development of a low-profile portable concrete barrier, Transportation Research Record no. 1367, Transportation Research Board, 1992.